

10. ASSESSMENT OF THE EFFECTS OF INLET SPILLAGE, BYPASS, AND  
BLEED AIR ON THE PERFORMANCE OF SUPERSONIC CRUISE AIRPLANES

By Lowell E. Hasel, Robert L. Weirich,  
and Vincent R. Mascitti  
NASA Langley Research Center

SUMMARY

The drags created by the overboard discharge of the excess inlet airflow during acceleration and of the inlet bleed air during cruise are critical factors in determining the performance of long-range supersonic cruise airplanes. Bypassing some of the excess air to the ejector during acceleration can reduce very significantly the excess air drag. Bleed drag reductions during cruise are attainable by tailoring of bleed and vortex-generator systems to increase the pressure recovery for a given bleed flow, by ducting flow to the ejector, and by surface injection to reduce the skin friction.

The cruise inlet pressure recovery which results in maximum airplane performance is strongly influenced by bleed drag. Unless the bleed drag can be made quite small, the potential performance benefits associated with operating the inlet at its maximum pressure recovery are not achievable.

INTRODUCTION

For long-range supersonic cruise airplanes such as the supersonic transport (SST) the payload is very sensitive to drag. Quite literally this situation has made it necessary to fight for every drag count and to examine closely potential methods of reducing each drag item. Such an examination must include the drags created by the discharge of the excess inlet and boundary-layer bleed air. In this paper these sources of drag are considered and known methods of reducing the associated performance penalties, either by optimization or drag reduction techniques, are reexamined. Few, if any, new concepts are suggested to those who are closely associated with the design of propulsion systems.

SYMBOLS

A	area, ft <sup>2</sup>
A <sub>c</sub>	inlet capture area, ft <sup>2</sup>
C <sub>v</sub>	nozzle velocity coefficient
D	drag, lb

F engine net thrust, lb  
 m airflow, lb/sec  
 M Mach number  
 $P_t$  total pressure, lb/ft<sup>2</sup>  
 q dynamic pressure, lb/ft<sup>2</sup>

Subscripts:

dis discharged air  
 2 engine face  
 $\infty$  free stream

INLET-ENGINE AIRFLOW MATCHING

As a starting point for this discussion the typical inlet-engine airflow matching characteristics for the supersonic transport are reviewed in figure 1. The ordinate is the conventional mass-flow ratio term in which the various airflow quantities, denoted by  $m$ , are referenced at each Mach number to  $m_{A_c}$ , the airflow in a stream tube with an area equal to the inlet area  $A_c$ . At the design Mach number of 2.7, the inlet is sized to satisfy the airflow requirements of the engine, cabin air-conditioning system (narrow unshaded strip), nozzle cooling, inlet boundary-layer bleed, and the bypass control system. At Mach numbers below the design value, the airflow requirements decrease significantly as shown by the lower heavy line. The amount of air delivered by the inlet also decreases, as indicated by the upper heavy line, because of the shock spillage ahead of the inlet lip. The inlet, however, supplies more air than the system requires and the excess air, which is called bypass in the figure, must be discharged overboard as illustrated in the left schematic sketch at the top of the figure.

Typical values of the drag coefficient which are created by discharging overboard the spillage, bypass, and inlet bleed air are shown in figure 2. The drag coefficient is based on the inlet area  $A_c$ . At cruise conditions,  $M_\infty = 2.7$ , most of the drag originates from the boundary-layer bleed air. At lower speeds, the drag coefficient is considerably larger and is primarily due to the spillage and bypass air. The drag level is equivalent to about 3 percent of the total airplane drag at cruise and to 8 or 9 percent at transonic speeds. If the bleed and bypass drag could be completely eliminated during the cruise portion of the flight, the total mission fuel consumption for a 500 000-pound SST airplane with typical aerodynamics would be reduced about 4500 pounds. This is a significant fuel saving when compared with the 40 000-pound payload. (A similar study is contained in ref. 1.) Elimination

of all the spillage, bypass, and bleed drag during the acceleration portion of the flight would reduce the fuel consumption by an additional amount of about 2000 pounds, or somewhat less than one-half of the 4500-pound cruise fuel increment. The acceleration fuel increment due to a given level of drag, such as that given in figure 2, can vary by large amounts, depending on the airplane and engine characteristics and the flight-path restrictions. The primary controlling factor is the thrust-minus-drag margin of the airplane. As the thrust-minus-drag margin decreases the fuel increment will increase. Generally, the acceleration fuel increment is small for the SST, but it can be large if the thrust-minus-drag margin becomes too small.

#### DRAG REDUCTION DURING ACCELERATION

Several approaches may be used to reduce the discharged-air drag during acceleration. (See refs. 2, 3, and 4.) At transonic speeds a trade-off is normally made between the amount of air spilled and bypassed so that the resultant drag is minimized. A primary problem here is the accurate assessment of the spillage drag because of the difficulty of determining the drag reduction due to suction forces on the lip and forward portion of the cowl. This subject is discussed in paper no. 12 by Anderson, Petersen, and Sorensen.

The excess-air drag may be significantly reduced by ducting a portion of the bypass air around the engine into the variable-area ejector nozzle. The reason that such an improvement can be achieved is shown in figure 3. The ordinate is an incremental force divided by the free-stream dynamic pressure and the free-stream tube area of the bypass air. When the air is discharged through a typical bypass nozzle, the drag coefficient indicated by the shaded area labeled "bypass nozzle" is produced. Analysis of data presented in reference 5 indicates that when the bypass air is discharged as secondary air through the engine ejector nozzle the nozzle performance may actually be improved and an increase in net thrust produced. The magnitude of the net thrust increase is indicated by the shaded area labeled "engine ejector nozzle." The net thrust-coefficient increment is largest at transonic speeds where the thrust-minus-drag margin is normally smallest. To illustrate the potential benefits of bypassing air to the nozzle, the discharged-air drag presented in figure 2 was recomputed for the case in which a portion of the bypass air (fig. 1) equal to 5 percent of the engine air was exhausted through the ejector nozzle. The lower drag level reduced the acceleration fuel consumption increment by about 40 percent.

Several comments should be made with regard to the use of the bypass air in the ejector nozzle. First, the amount of air which can be efficiently used in this manner will be determined by the nozzle pumping characteristics. At present only a limited amount of data is available for determining these characteristics for high-efficiency nozzles. Second, ducting the bypass air around the engine to the nozzle will probably require an increase in frontal area of the nacelle and an increase in nacelle weight. However, because of the favorable wing-nacelle interference effects which are known to be achievable during cruise, the increase of nacelle frontal area will not necessarily result in an adverse effect on overall performance.

## OPTIMIZATION OF INLET PERFORMANCE DURING CRUISE

It may be recalled from the previous discussion that during the cruise portion of the flight the total mission fuel increment attributable to bleed and bypass drag was about 4500 pounds. About three-fourths of this fuel increment, or 3400 pounds, is due to the bleed drag.

One approach to the bleed drag problem is to make a trade-off between inlet pressure recovery and bleed drag so that airplane performance is maximized. A thorough optimization of this type involves a complex procedure but the basic concept can be illustrated by the very simplified method outlined as follows (see also ref. 6):

Objective: Minimize fuel flow

$$\text{Fuel flow} = \text{Thrust} \times \text{Specific fuel consumption}$$

$$\text{Thrust} = D_{\text{basic airplane}} + D_{\text{bypass}} + D_{\text{bleed}}$$

$$\text{Specific fuel consumption} = f\left(\text{Thrust}, \frac{P_{t,2}}{P_{t,\infty}}\right)$$

Since the airplane is at cruising conditions the performance may be judged on the basis of fuel flow. Hence, the objective is to minimize the fuel flow. In other words, the product of thrust and specific fuel consumption must be minimized. Since thrust must equal drag the thrust is equal to the sum of the drag of the basic airplane (which does not change with pressure recovery) and the drag of the bleed and bypass flows. Specific fuel consumption is a function of the thrust and the inlet pressure recovery.

This procedure can be further understood by the use of the typical set of inlet-pressure-recovery data (fig. 4) which were obtained by the Ames Research Center at a Mach number of 3. Inlet pressure recovery is plotted as a function of inlet mass-flow ratio. The inlet is an axisymmetric design. The boundary-layer-bleed configuration consists of annular rows of holes located on the centerbody and cowl in the supersonic diffuser and at the inlet throat. The bleed air from the centerbody passes through struts to reach the external surface of the nacelle. Bleed mass-flow and pressure recovery were measured for each of these four sets of bleed holes concurrent with the inlet recovery and mass-flow measurements. The data presented in figure 4 indicate that as the pressure recovery decreases the bleed flow decreases. Hence the bleed drag and the required engine thrust decrease. On the other hand, the engine specific fuel consumption increases as pressure recovery decreases. Since the specific fuel consumption and thrust vary in opposite directions as the pressure recovery changes a minimization of the fuel flow may be possible.

It should be mentioned that in an optimization of this type the inlet size decreases as the pressure recovery decreases because the inlet is sized at each value of pressure recovery to match the decreasing airflow requirements of the engine, bleed system, and bypass control system (2 percent of inlet flow). For

example, in the optimization study which follows only the portion of the curve in figure 4 extending from pressure-recovery values of 0.923 to 0.887 is considered. The corresponding reduction in inlet capture area is 6.4 percent.

The drag created by discharging the bleed air depends on the exit nozzle configuration. (See appendix.) The drag values presented as a function of inlet pressure recovery in figure 5 were calculated by assuming that the air was discharged through four sonic nozzles with nozzle velocity coefficients of 0.985. The total pressure of the bleed air removed from the supersonic diffuser varied from 0.12 to 0.20 of the free-stream total pressure. The corresponding values for the air removed from the inlet throat region varied from about 0.24 to 0.43. The amount of bleed air was established by sizing the inlet to supply the air required by typical SST turbojet and turbofan engines operating at 65 000 feet. At the highest inlet pressure recovery the bleed drag is about 1130 pounds for the turbofan engine and 800 pounds for the turbojet. These values decrease about 20 percent when the design inlet pressure recovery decreases from 0.923 to 0.887.

The bypass-control-air drag was computed in a similar manner by assuming a pressure-recovery value of 0.95 of the inlet recovery. These drag values (not presented in fig. 5) are about 14 percent of the bleed-drag values at the highest pressure recovery and decrease slightly as the pressure recovery is reduced because of the decreasing inlet size.

The fuel flow variations for both engines are shown in figure 6. Fuel flow, expressed in pounds/hour/engine, is plotted as a function of inlet pressure recovery. The basic airplane drag, which does not vary with inlet pressure recovery, has been assumed to be equal to the minimum augmented or 10-percent augmented thrust output of each engine at an inlet pressure recovery of 0.923. The fuel flow of the turbofan engine is essentially constant over the range of inlet pressure recoveries considered. There is some increase in the turbojet fuel flow as pressure recovery decreases. This increase is larger for the 10-percent augmented case and amounts to about 220 pounds/hour/engine. The results of a complete optimization would account for other effects, such as inlet weight and skin-friction drag, spillage and bypass-air drag during acceleration, and nacelle-airframe wave-drag interference. Inclusion of these effects could very well alter the fuel-flow curves to favor, more than is shown in figure 6, the inlet designed for operation at the lower pressure recoveries. The point to be made from these curves is that a significant performance penalty does not necessarily result when the propulsion system is designed to operate at less than the maximum recovery attainable with a given inlet. Furthermore, other factors, such as internal-flow stability and hot-day operation, may be improved by the selection of the lower recoveries as the design point.

It is of interest to carry the study one step further and note the effect on fuel flow of increasing the inlet maximum pressure recovery (fig. 7) by reducing the back pressure on the throat boundary-layer bleed holes. The discussion thus far has been based on a configuration which attained a maximum pressure recovery of 0.923. Decreasing the back pressure increased the maximum pressure recovery to 0.934 and increased the amount of bleed at a given recovery.

The corresponding fuel-flow curves for the turbojet engine are shown in figure 8. At a given value of pressure recovery the fuel flow is less for the inlet which has the lower maximum recovery. This difference would be expected because of the lower bleed flows of this inlet. The most interesting point to note in figure 8 is that the minimum fuel flow of the higher recovery inlet exceeds that of the lower recovery inlet over most of the pressure recovery range considered. Admittedly the differences are small but the point can nevertheless be made that the best inlet for a cruise vehicle cannot be selected solely on the basis of maximum attainable pressure recovery. As will be emphasized later, one should not conclude from this analysis that the attainment of high pressure recovery is not an important inlet research goal. The research challenge is to obtain the high recoveries with low rates of bleed flow. This may be accomplished by such methods as detailed tailoring of the bleed system and of the vortex-generator patterns in the subsonic diffuser. This area of research is discussed in paper no. 11 by Sorensen, Anderson, Wong, and Smeltzer.

As is discussed more completely in the appendix, the slope and level of the fuel-flow curves (fig. 8) are dependent on the relationship between bleed drag and inlet pressure recovery. For example, if the bleed drag could be completely eliminated the fuel-flow level would be lower and the variation with pressure recovery would be greater than for the cases previously discussed. At the high recoveries the level is decreased by about 7 percent. A comparison of these curves emphasizes the importance of minimizing the bleed drag. Reduction of the bleed drag allows more of the potential benefits due to the higher inlet pressure recoveries to be realized.

#### DRAG REDUCTION DURING CRUISE

One potential method of reducing the bleed drag which is independent of inlet improvements is to duct the air around the engine and discharge it into the ejector nozzle. The associated drag penalty is shown in figure 9. In this figure the drag of the bleed air referenced to the free-stream dynamic pressure and the free-stream tube area of the bleed air is plotted as a function of bleed-air pressure recovery. The drag coefficient produced by discharging the air through a sonic nozzle is shown by the solid line. The shaded area indicates the drag which might result from discharging the air through the engine ejector nozzle. This area is bounded by the performance of two typical, high efficiency, SST nonafterburning nozzle configurations. (See ref. 5.) It appears possible that with a proper nozzle design the bleed air might be discharged with no significant drag penalty.

In paper no. 30, Peterson and Monta discuss injection of the bleed air into the nacelle boundary layer in such a manner that the nacelle skin friction is reduced. Based on the limited amount of data now available (ref. 7) the drag coefficient which results from using the air in this manner at a Mach number of 3 is about 0.2 to 0.3. The research conducted to date, however, has not been adequate to predict the maximum drag reductions attainable by this technique.

## CONCLUDING REMARKS

Critical drag items are the drag created by the overboard discharge of the excess airflow during acceleration and the discharge of the inlet bleed flow during cruise. If the bleed flow is discharged overboard in a conventional manner the associated total mission fuel consumption increment is about 3400 pounds for a typical SST configuration.

Bypassing air to the ejector during acceleration is an efficient method for disposal of the excess airflow. This method of drag reduction is of particular interest when the acceleration thrust-minus-drag margin is small.

The cruise inlet pressure recovery which results in maximum airplane performance is strongly influenced by bleed drag. Unless the bleed drag can be made quite small, the potential performance benefits associated with operating the inlet at its maximum pressure recovery are not achievable.

Bleed drag reductions during cruise are attainable by tailoring of bleed and vortex-generator systems to increase the pressure recovery for a given bleed flow, by ducting flow to the ejector, and by surface injection to reduce skin friction. All these approaches have merit, and use of them should result in improvements in overall airplane performance.

## APPENDIX

### INSTALLED DRAG OF DISCHARGED-AIR NOZZLES

The drag created by discharging air from various types of nozzles has been studied both theoretically and experimentally (refs. 8 to 13). References 8 and 9 consider the problem in detail and correlate the measured drags with drags predicted from pressure distributions calculated by the method of characteristics. By using the data presented in reference 8 and extending the method when necessary the drag characteristics of a series of representative nozzles have been calculated at  $M_{\infty} = 2.94$  and are presented in figure 10. The drag is referenced to the free-stream tube area of the air being discharged and is plotted as a function of the total pressure recovery of the discharged air. The local external flow was assumed to be at free-stream conditions. These drag characteristics include all the thrust and pressure forces acting on the nozzle surfaces and the pressure forces on the external surface of the door. The nozzle velocity coefficient was assumed to be 1 for all configurations. The flush and axial configurations have no door drag. The axial sonic and axial complete-expansion nozzles are included for reference purposes since, in the past, these configurations have been a convenient basis for determining discharged-air drag.

Two practical sonic nozzle configurations are considered in figure 10. For both the flush and external door designs the flow is discharged at a  $5^{\circ}$  angle and the sonic throat was assumed to be located at the lip which terminates the upper surface or door. Both of these nozzles result in drag levels which are higher than that of the axial sonic nozzle.

The partly submerged, complete-expansion nozzle discharging at a  $5^{\circ}$  angle is an optimum design for  $5^{\circ}$  fully expanded nozzles. At values of total pressure recovery less than 0.25 its drag is greater than that of the axial sonic nozzle. At high values of total pressure recovery use of this type of nozzle results in a drag level which is quite low.

The optimization study presented in figure 6 was based on the bleed and bypass drag generated by axial sonic nozzles with a nozzle velocity coefficient of 0.985. Most of the discharged-air drag is created by the bleed air which had pressure-recovery values from 0.12 to 0.43. Hence, the assumption of sonic nozzle drag is reasonable, although the resultant drags may tend to be somewhat too large.

Figures 11 and 12 have been prepared to indicate the effects which the assumptions regarding the bleed and bypass drags may have on the optimization results presented in figure 6. Figure 11 is a comparison of the bleed drag for the sonic and complete-expansion nozzles. (It should be noted that the complete-expansion nozzle underestimates the discharged-air drag and may therefore be thought of as a limit-type curve.) The assumption of a complete expansion nozzle decreases the bleed drag at the highest recovery by about 36 percent and also reduces the slope of the drag curve. The corresponding fuel-flow

curves for the turbojet engine are compared in figure 12. The complete-expansion-nozzle assumption decreases the fuel flow at a given value of inlet pressure recovery, as would be expected, and the fuel flow increases at a more rapid rate as the design inlet pressure recovery is reduced.

Figure 12 indicates quite clearly that the slope and level of the fuel-flow curves are dependent on the relationship between bleed-air drag and inlet pressure recovery. As the bleed drag for a given inlet is reduced the slopes of the fuel-flow curves change in such a manner that the optimum recovery tends to approach the maximum value. It must be remembered, however, that when a complete optimization is made this trend may not be as definite as shown in figure 12.

## REFERENCES

1. Anderson, Warren E.; and Nelms, Walter P., Jr.: Performance and Control of Air-Induction Systems for a Commercial Supersonic Transport - Part I. Geometry and Steady-State Performance. Proceedings of the AIAA/ASD Meeting on Future Aerospace Vehicles - The Challenge to Interdisciplinary Concepts, ASD TDR 64-76, Apr. 1964, pp. 250-265.
2. Hearth, Donald P.; and Connors, James F.: A Performance Analysis of Methods for Handling Excess Inlet Flow at Supersonic Speeds. NACA TN 4270, 1958.
3. Hearth, Donald P.: Use of Main-Inlet Bypass To Supply Ejector Exhaust Nozzle at Supersonic Speeds. NACA RM E56K08, 1957.
4. Davis, Wallace F.; and Scherrer, Richard: Aerodynamic Principles for the Design of Jet-Engine Induction Systems. NACA RM A55F16, 1956.
5. Stofan, Andrew J.; and Mihalow, James R.: Performance of a Variable Divergent-Shroud Ejector Nozzle Designed for Flight Mach Numbers up to 3.0. NASA TM X-255, 1961.
6. Weber, Richard J.; and Luidens, Roger W.: A Simplified Method for Evaluating Jet-Propulsion-System Components in Terms of Airplane Performance. NACA RM E56J26, 1956.
7. Peterson, John B., Jr.; McRee, Donald I.; Adcock, Jerry B.; and Braslow, Albert L.: Further Investigation of Effect of Air Injection Through Slots and Porous Surfaces on Flat-Plate Turbulent Skin Friction at Mach 3. NASA TN D-3311, 1966.
8. Anderson, D. C.: Efficiency of Flush and Protruding Oblique Exhaust Nozzles With and Without External Flow. R-0955-22 (Contract NOa(s)55-133-c), Res. Dept., United Aircraft Corp., Oct. 1957.
9. Cnossen, J. W.: Efficiency of Flush Oblique Nozzles Exhausting into Supersonic Streams Having Mach Numbers up to 4. R-1285-10 (Contract NOa(s) 55-133-c), Res. Dept., United Aircraft Corp., Sept. 1959.
10. Nelson, William J.; and Dewey, Paul E.: A Transonic Investigation of the Aerodynamic Characteristics of Plate- and Bell-Type Outlets for Auxiliary Air. NACA RM L52H20, 1952.
11. Dewey, Paul E.: A Preliminary Investigation of Aerodynamic Characteristics of Small Inclined Air Outlets at Transonic Mach Numbers. NACA TN 3442, 1955. (Supersedes NACA RM L53C10.)
12. Dewey, Paul E.; and Vick, Allen R.: An Investigation of the Discharge and Drag Characteristics of Auxiliary-Air Outlets Discharging Into a Transonic Stream. NACA TN 3466, 1955.

13. Vick, Allen R.: An Investigation of Discharge and Thrust Characteristics of Flapped Outlets for Stream Mach Numbers From 0.40 to 1.30. NACA TN 4007, 1957.

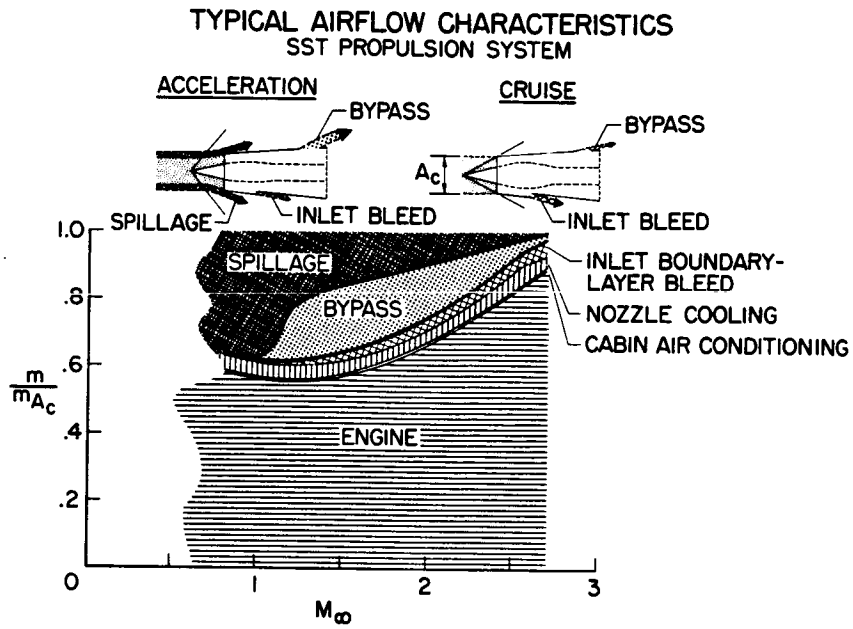


Figure 1

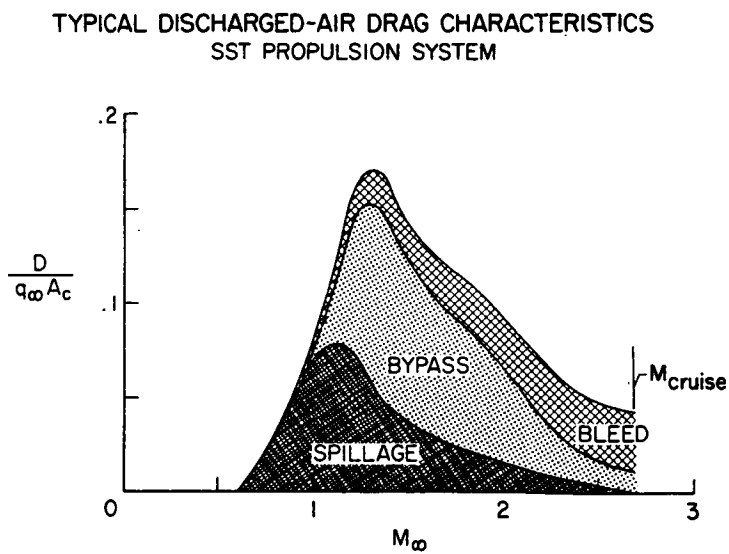


Figure 2

DRAG REDUCTION DURING ACCELERATION  
BYPASS AIR

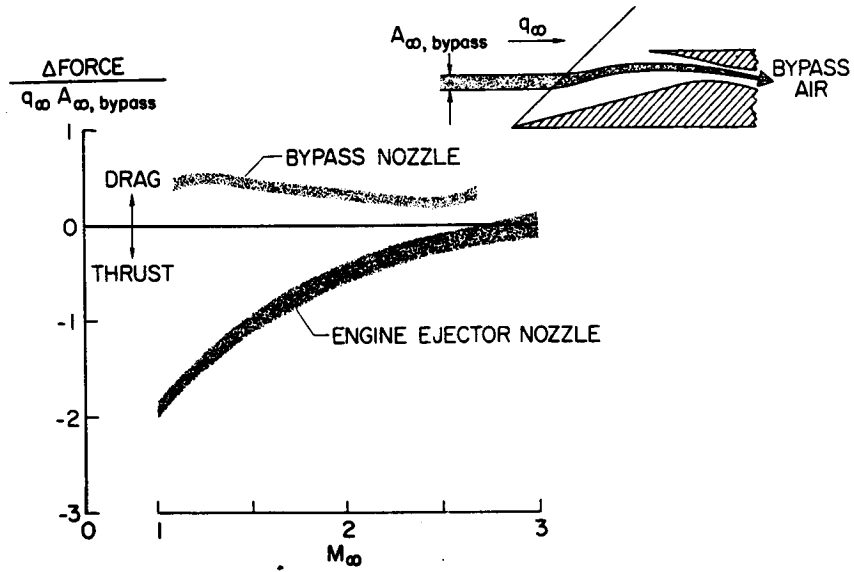


Figure 3

AXISYMMETRIC-INLET PERFORMANCE  
TYPICAL BLEED-HOLE CONFIGURATION;  $M_\infty = 3$

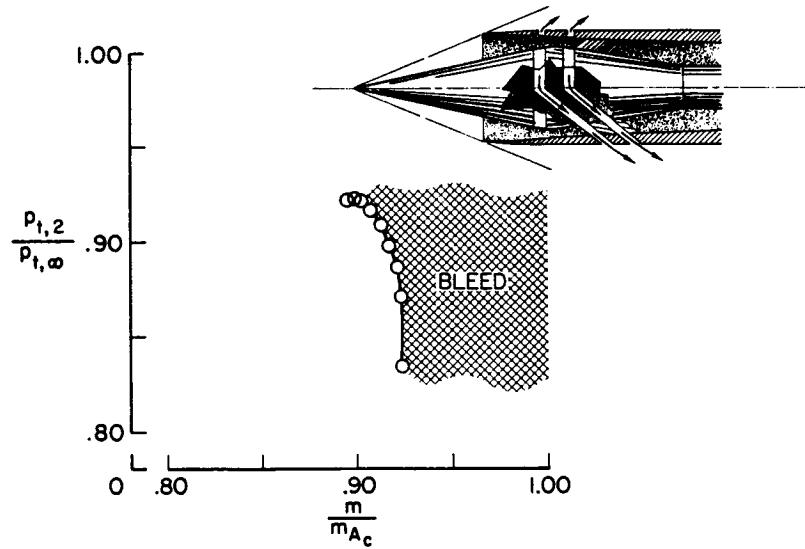


Figure 4

CALCULATED BLEED-AIR DRAG  
SONIC NOZZLE;  $C_v = 0.985$ ;  $M_\infty = 3$

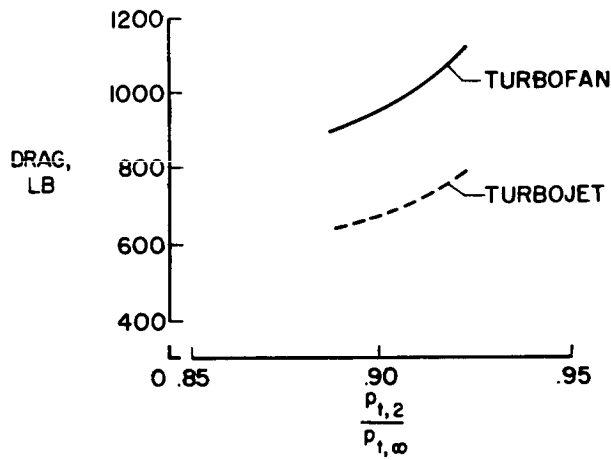


Figure 5

INLET OPTIMIZATION  
TYPICAL BLEED-HOLE CONFIGURATION;  
SONIC BLEED NOZZLE;  $C_v = 0.985$ ;  $M_\infty = 3$

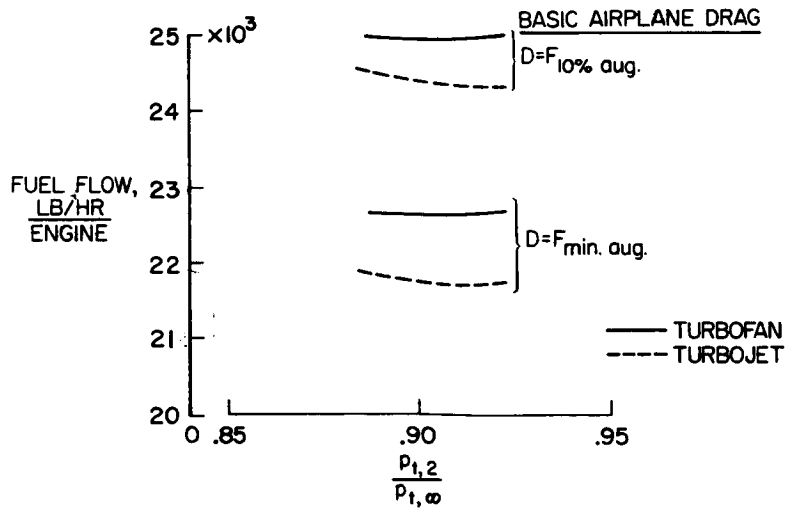


Figure 6

AXISYMMETRIC-INLET PERFORMANCE  
EFFECT OF BLEED-HOLE BACK PRESSURE;  $M_\infty=3$

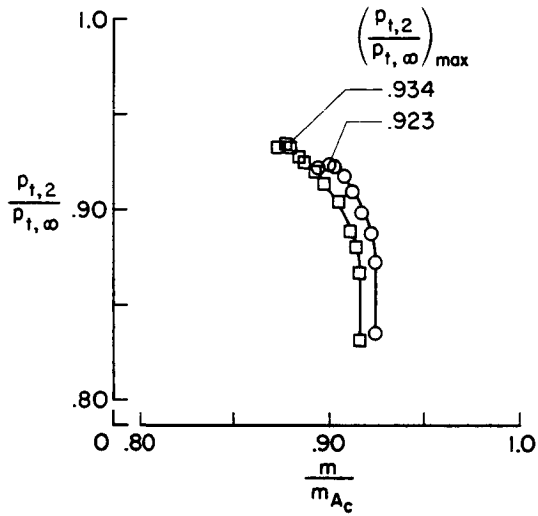


Figure 7 .

INLET OPTIMIZATION  
EFFECT OF BLEED-HOLE BACK PRESSURE; TURBOJET ENGINE;  
SONIC EXIT NOZZLE;  $C_V=0.985$ ;  $M_\infty=3$

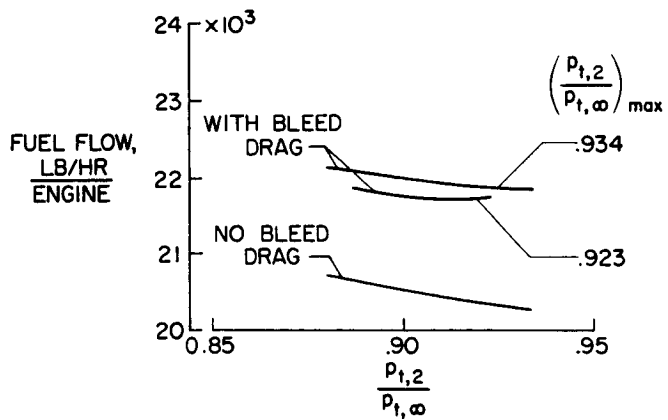


Figure 8

DRAG REDUCTION DURING CRUISE  
INLET BLEED AIR;  $M_\infty = 3$

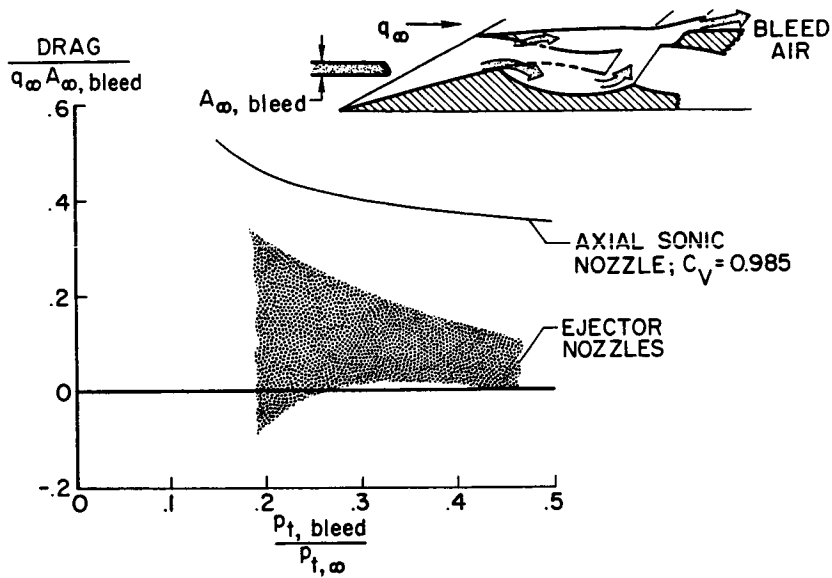


Figure 9

INSTALLED DRAG OF DISCHARGED-AIR NOZZLES  
 $M_\infty = 2.94$

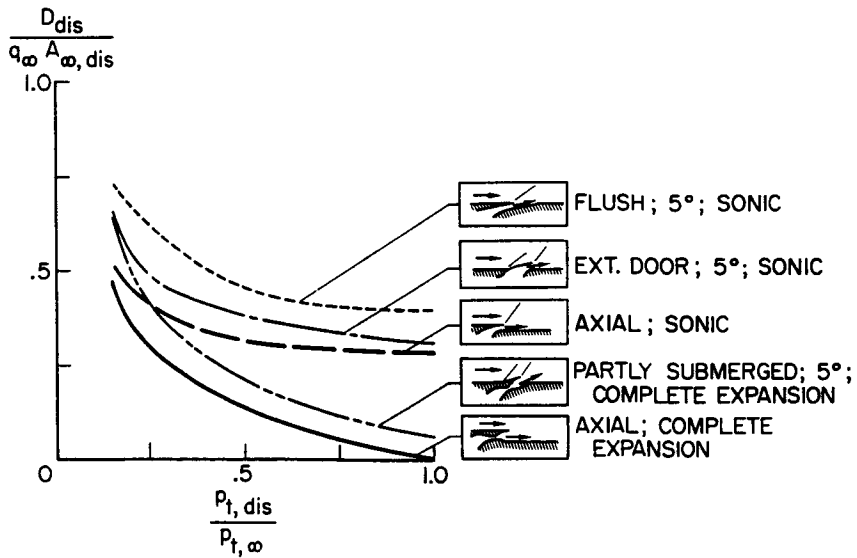


Figure 10

**CALCULATED BLEED-AIR DRAG  
EFFECT OF EXIT-NOZZLE CONFIGURATION;  
TURBOJET ENGINE;  $M_\infty=3$ ;  $C_v=0.985$**

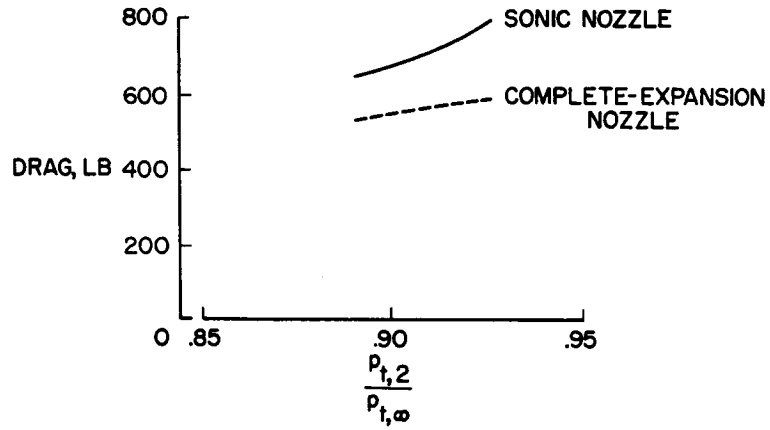


Figure 11

**INLET OPTIMIZATION  
EFFECT OF EXIT-NOZZLE CONFIGURATION;  
TURBOJET ENGINE;  $M_\infty=3$ ;  $C_v=0.985$**

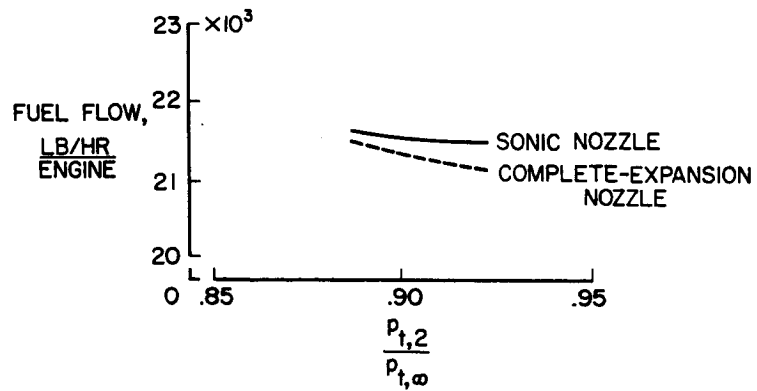


Figure 12